Available online at www.sciencedirect.com

jmr&t Journal of Materials Research and Technology

journal homepage: www.elsevier.com/locate/jmrt

Original Article

Desulfurization behavior of Si-killed 316L stainless steel melt by CaO-SiO_2-CaF_2-Al_2O_3-MgO slag

Tae Su Jeong [a], *Jin Hyung Cho* [a,b], *Jung Ho Heo* [a,c], *Joo Hyun Park* [a,*]

[a] *Department of Materials Science and Chemical Engineering, Hanyang University, Ansan, 15588, South Korea*
[b] *Technical Research Laboratory, Hyundai Steel, Dangjin, 31719, South Korea*
[c] *Department of Materials Engineering, KU Leuven, Kasteelpark Arenberg 44, Leuven, 3001, Belgium*

ARTICLE INFO

Article history:
Received 26 January 2022
Accepted 7 March 2022
Available online 24 March 2022

Keywords:
Stainless steel
Sulfide capacity
Mass transfer coefficient
Kinetics
Viscosity
Basicity

ABSTRACT

The desulfurization behavior of 316L stainless steel (STS316L) melt with the CaO-SiO_2-CaF_2-Al_2O_3-MgO slag was investigated with different CaO/SiO_2 (=C/S) ratio and CaF_2 content at 1873 K. As the C/S ratio increased, the sulfide capacity increased, whereas the sulfide capacity of the high C/S (=1.7) slag was not affected by CaF_2 content. The overall mass transfer coefficient (k_O) increased with C/S ratio, but was constant above a critical C/S value, and it was also constant across varied CaF_2 content at relatively high C/S (=1.7) condition. Since the metal condition of the present study was constant, the change in k_O was caused by slag phase mass transfer coefficient (k_s) and sulfur distribution ratio (L_S), which were affected by the physicochemical properties of the slag. Since desulfurization reaction requires consideration of both kinetic and thermodynamic factors, the '$\log C_{S^{2-}} - \log \eta$' (where $C_{S^{2-}}$ is sulfide capacity and η is viscosity), was proposed as a meaningful physicochemical parameter. If the slag basicity is relatively high, at which the k_O is equivalent regardless of slag compositions, the desulfurization reaction is controlled by metal phase mass transfer. However, if the slag basicity becomes lower, at which the k_O significantly decreases, the desulfurization reaction is assumed to be controlled by slag phase mass transfer and/or mixed controlled process.

1. Introduction

Due to their high corrosion resistance, stainless steel products are widely used across industries from manufacturing process to construction and transportation. However, the product performance can be significantly affected by the steel cleanliness, e.g., the nonmetallic inclusion number density, size distribution, morphology and chemistry [1,2]. Since sulfur in steel hardly dissolves in austenite matrix at low temperatures, most of it is precipitated as sulfides (Fe, Mn)S at grain boundaries. When the sulfur concentration in the steel increases, the quantity of sulfides segregating at grain boundaries inevitably increases, and thus the hot workability, corrosion resistance and impact toughness of the steel are reduced, which adversely affects the quality of the steel [3–5]. Therefore, it is essential to control the concentration of sulfur

* Corresponding author.
E-mail address: basicity@hanyang.ac.kr (J.H. Park).
https://doi.org/10.1016/j.jmrt.2022.03.048

in molten steel, and slag chemistry is also very important since sulfur is removed *via* slag-metal reaction.

The desulfurization reaction by slag proceeds by a reducing reaction in which S in molten steel is replaced with S^{2-} ion in the slag through an electrochemical reaction with oxygen ion in the slag and can be expressed as Eq. (1) [6,7].

$$[S] + (O^{2-}) = [O] + (S^{2-}) \quad (1)$$

Typically, the CaO-SiO_2-Al_2O_3–based slags are used and MgO is added to prevent excessive corrosion of the MgO(–C) type ladle lining [8–10]. Since CaO, a representative basic oxide, predominantly participates in desulfurization of molten steel, the relationship between empirical basicity index (CaO/SiO_2 or CaO/Al_2O_3 ratio) and desulfurization efficiency has been studied by many researchers [6,7,11–15]. Fincham and Richardson [6] defined the sulfide capacity ($C_{S^{2-}}$) and plotted the relationship between the sulfide capacity and the molar fraction of basic oxides (CaO, MgO or FeO) in molten slags, and drew the iso-sulfide capacity contour on the CaO-SiO_2-Al_2O_3 phase diagram at 1923 K. Their results indicate that the sulfide capacity increases with CaO content. Similar results were reported by Hino et al. [13] The sulfide capacity increased with temperature, whereas it decreased with the increase of SiO_2 content even in CaO-saturated slag.

Andersson et al. [14] calculated the sulfide capacity of the CaO-Al_2O_3-8%MgO-7%SiO_2 slags by using the KTH model and concluded that the sulfide capacity as well as sulfur distribution ratio (L_S) increased with an increase of the CaO/Al_2O_3 ratio in the slag. Bronson and Pierre [11] determined the sulfide capacity of the CaO-SiO_2-CaF_2 (or B_2O_3) slags by the encapsulation method at 1773 K and concluded that the sulfide capacity increased with increasing content of CaF_2, whereas it decreased with increasing content of B_2O_3. In their work, CaF_2 was believed to depolymerize silicate network as given in Eq. (2) for example, resulting in an increase of free oxygen (O^{2-}) in the slag [11,15–17].

$$(Si_3O_9)^{6-} + (F^-) = (Si_3O_8F)^{5-} + (O^{2-}) \quad (2)$$

Susaki et al. [12] also measured the sulfide capacity of the CaO-CaF_2-SiO_2 slag at 1573 K through metal-slag-gas equilibrium experiments and found that the sulfide capacity increased with increasing Al_2O_3 content by substituting SiO_2 because SiO_2 was more acidic than Al_2O_3 in the CaO-based slag. The structure of aluminosilicate melts with or without CaF_2 was thoroughly investigated by the present authors [16–19].

Meanwhile, the desulfurization kinetics has been investigated by several researchers [13,20–25]. In general, when the desulfurization of molten iron is performed using highly basic slags with high sulfide capacity, the mass transfer of sulfur in the metal phase is known to be a rate controlling step (RCS) for desulfurization because of the high sulfur distribution ratio as well as the relatively fast interfacial chemical reaction at steelmaking temperatures [20–23]. However, several researchers have suggested that the slag phase mass transfer can be the RCS for desulfurization process [24,25]. Jung and Pak [25] conducted a desulfurization experiment of carbon-saturated iron using the CaO-SiO_2-CaF_2 slag at 1623 K and concluded that the sulfur removal reaction was controlled by the slag phase mass transfer. They explained that as the CaO/SiO_2 ratio increased, high sulfide capacity in conjunction with low viscosity slags were secured and the desulfurization rate improved. The similar results were reported by Choi et al. [24] from the desulfurization experiments of molten pig iron using the CaO-SiO_2-Al_2O_3-Na_2O quaternary slag at 1623 K.

Alternatively, Kang et al. [26] conducted a desulfurization experiment of (Al-killed) molten steel using the CaO-Al_2O_3-SiO_2-MgO-CaF_2 slag at 1823 K and observed that the sulfur distribution ratio increased with increasing CaO/SiO_2 or CaO/Al_2O_3 ratios of slag. It was found that when highly basic slags having a sulfur distribution ratio of 400 or more were used (i.e., $L_S \geq 400$), the metal phase mass transportation of sulfur was found to be the RCS for sulfur removal process. However, when the relatively less basic slags were employed, the overall mass transfer coefficient of sulfur significantly decreased due to poor physicochemical properties of slag such as low sulfur distribution ratio in conjunction with high viscosity, and thus the transition of RCS for sulfur removal reaction occurred from metal phase mass transfer to slag phase mass transfer or mixed phase controlled process.

A desulfurization experiment of (Al-killed) molten steel was also conducted by the present authors using the CaO-Al_2O_3-SiO_2-MgO slag at 1823 K to compare the influence of various fluxing materials such as fluorspar, red mud, ferromanganese slag and white mud [27,28]. It was proposed that '$\log C_{S^{2-}} - \log\eta$' index could be a good parameter to evaluate the combinatorial effect of the physicochemical properties of slag on the desulfurization rate.

Although the desulfurization behavior of hot metal and carbon steel using various slags has been investigated by many researchers, there are few studies on the desulfurization kinetics of Si-killed stainless steel melts. Yan et al. [29] conducted desulfurization experiments of austenitic stainless steel using CaO-Al_2O_3–based slags from 1873 to 1923 K. They observed that the sulfur distribution ratio and average S removal rate increased with the CaO/Al_2O_3 ratio and developed a desulfurization kinetic model based on the two film theory. Nevertheless, it is hard to find the fundamental studies regarding the effect of slag composition on the desulfurization kinetics of Si-killed stainless steel melts, even though there are bunch of studies on the cleanliness and inclusion engineering in stainless steels [1,2,30–33].

Therefore, in the present study, a desulfurization experiment of Si-killed stainless steel (STS 316L grade) melt using CaO-SiO_2–based slags (i.e., CaO-SiO_2-CaF_2-5%Al_2O_3-5%MgO) was performed. In order to consider thermodynamic and thermophysical properties of slag, the CaO/SiO_2 ratio and CaF_2 content were set as experimental variables, respectively. Thereafter, the influence of the physicochemical properties according to the slag composition on the desulfurization efficiency of STS 316L melt was investigated.

2. Experimental procedure

The experimental apparatus used to study desulfurization behavior of stainless steel melt are shown in Fig. 1. To remove impurities from the quartz reaction chamber, a rotary vane pump was used. The chamber was then filled with a high-

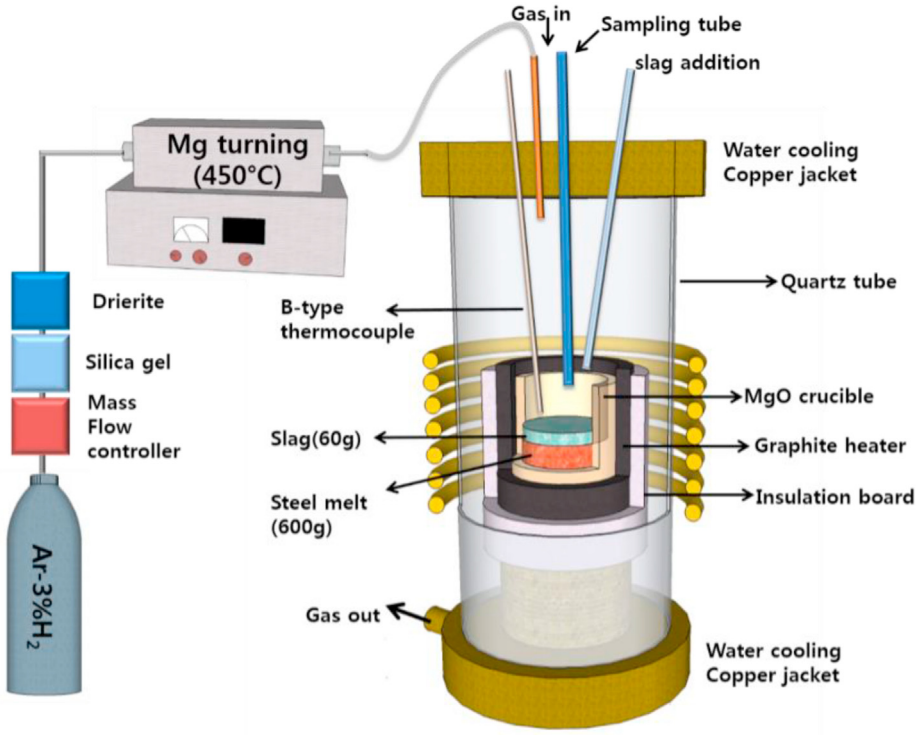

Fig. 1 – Schematic diagram of the experimental apparatus.

purity Ar–3%H_2 gas mixture, using a mass flow controller. The STS 316L (Fe–16Cr –12Ni–2Mo–0.3Si–0.5Mn–0.03S, wt%, 600 g) was loaded in a fused magnesia crucible (outer diameter, OD: 60 mm, inner diameter, ID: 50 mm, and height, HT: 120 mm) for induction heating with a graphite heater (OD: 80 mm, ID: 65 mm, and HT: 120 mm), which was surrounded by an insulating material. Impurities in the gas mixture were removed by purification through Drierite (W.A. Hammond Drierite Co. Ltd., Xenia, OH), soda lime, silica gel (medium granular, 5–10 mesh), and Mg turnings at 723 K.

The experimental temperature was 1873 K, which was kept to within ±2 K using a B-type (Pt–30%Rh/Pt–6%Rh) thermocouple and a proportional integral differential controller. After the temperature stabilized, the pre-fused slag was added onto the surface of the molten steel through the quartz tube under an Ar–3%H_2 gas atmosphere. The synthetic slag was prepared by melting reagent-grade CaO, SiO_2, CaF_2, Al_2O_3, and MgO in a vertical resistance tube furnace in purified Ar atmosphere. CaO was prepared by calcination of $CaCO_3$ in air at 1273 K for 12 h. In order to understand the effect of basicity on the desulfurization efficiency, CaO/SiO_2 (= 1.0 to 2.3) ratio was considered to be an experimental variable. Also, the content of CaF_2 (= 10 to 30 wt%) was examined to confirm the effect of slag fluidity on desulfurization kinetics. The compositions of the slags are listed in Table 1 and shown in the CaO-SiO_2-CaF_2-5%Al_2O_3-5%MgO pseudo-ternary phase diagram calculated using FactSage™ software (ver. 7.3) as shown in Fig. 2.

Suction sampling to obtain steel samples and water quenching were conducted with a quartz tube (ID: 4 mm), and slag samples were obtained using a steel rod combined with nuts during the metal–slag reaction at 1873 K. Samples were collected at several times (0, 5, 10, 30, and 60 min). After the experiments were finished, the sulfur content of the metal and slag samples were obtained using a combustion analyzer (ELTRA, CS-800). The compositions of the steel and slag samples were determined by means of X-ray fluorescence spectroscopy (XRF; ZSX Primus IV, Rigaku) and inductively coupled plasma atomic emission spectrometry (ICP-AES; Spectro Arcos).

Table 1 – Compositions of slag used in the present study (wt%) and solid fraction.

Slag conditions		CaO	SiO_2	Al_2O_3	MgO	CaF_2	Mass fraction (Solid phase)
Fixed CaF_2 (=10wt%)	C/S = 1.0	40	40	5	5	10	–
	C/S = 1.3	48	32	5	5	10	–
	C/S = 1.7	50	30	5	5	10	0.08 (Ca_2SiO_4)
	C/S = 2.3	56	24	5	5	10	0.02 (Monoxide)
Fixed C/(S + A) ratio (=1.5)	15 CaF_2	47	28	5	5	15	–
	20 CaF_2	44	26	5	5	20	–
	25 CaF_2	41	24	5	5	25	–
	30 CaF_2	38	22	5	5	30	–

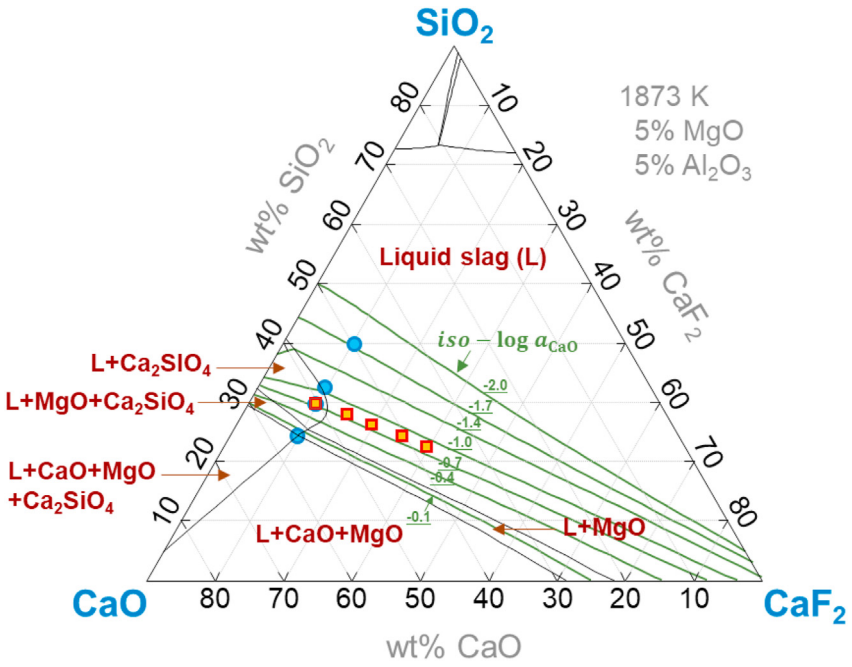

Fig. 2 – Experimental composition of the mixed slag used in the current study with iso-activity of CaO, as represented in the CaO-SiO_2-CaF_2-5%Al_2O_3-5%MgO phase diagram at 1873 K, calculated using FactSage™ 7.3 software.

3. Results and discussion

3.1. *Thermodynamics of the effect of CaO/SiO_2 ratio and CaF_2 content on desulfurization efficiency of STS316L melt*

The desulfurization ratio, i.e., $[wt\%S]_{t=t}/[wt\%S]_{t=0}$, in the molten steel was determined as a function of reaction time for various slag conditions such as CaO/SiO_2 (=C/S) ratio (Fig. 3(a)), and CaF_2 content (Fig. 3(b)). In most cases, a large amount of sulfur was removed within 15 min, and the sulfur concentration remaining in the molten steel after the 60 min experiment was low, approx. 14 (±4) ppm as listed in Table 2. However, the initial sulfur removal rate of the low basicity conditions (C/S ≤ 1.3) was relatively low compared to the rate of the other conditions and the concentration of sulfur remaining in the molten steel after the 60 min was relatively high, i.e., about 40–90 ppm as listed in Table 2.

The sulfur distribution ratio ($= L_S = (wt\%S)_{slag}/[wt\%S]_{metal}$) between STS 316L and slag melts at 1873 K are represented in Fig. 4. The L_S value sharply increases with increasing C/S ratio greater than 1.7, whereas it is not affected by the content of CaF_2 at C/S = 1.7 condition. The similar tendencies are also available in the literature [26–28]. In the present study, the high basicity slags are composed of multiphase system (Table 1), i.e., liquid + solid (8 wt% Ca_2SiO_4 for C/S = 1.7 or 2 wt% (Ca, Mg)O monoxide for C/S = 2.3), calculated using the FactSage™ (ver. 7.3) with FToxid database, which is a commercial thermochemical computing software widely used to predict the solid-liquid-gas multiphase reaction equilibria in ferrous- and

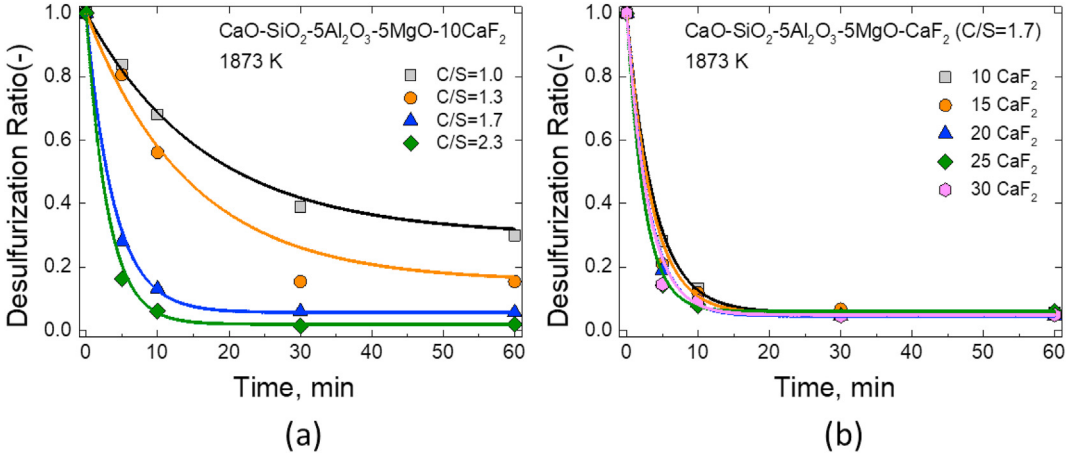

Fig. 3 – Desulfurization ratio as a function of reaction time for different (a) CaO/SiO_2 ratio and (b) CaF_2 content in the slag at 1873 K.

Table 2 – Sulfur content in steel (0, 5, 10, 30 and 60 min) and slag (60 min), and sulfur distribution ratio at 60 min.

Slag conditions		$[\%S]_0$	$[\%S]_5$	$[\%S]_{10}$	$[\%S]_{30}$	$[\%S]_{60}$	$(\%S)_{60}$	L_S
Fixed CaF_2 (=10wt%)	C/S = 1.0	0.0290	0.0245	0.0200	0.0110	0.0090	0.196	20 (±2)
	C/S = 1.3	0.0270	0.0220	0.0150	0.0040	0.0040	0.269	65 (±6)
	C/S = 1.7	0.0290	0.0080	0.0040	0.0020	0.0020	0.399	210 (±15)
	C/S = 2.3	0.0280	0.0050	0.0020	0.0006	0.0006	0.412	710 (±42)
Fixed C/(S + A) ratio (=1.5)	15 CaF_2	0.0280	0.0060	0.0030	0.0020	0.0015	0.343	230 (±27)
	20 CaF_2	0.0290	0.0055	0.0025	0.0010	0.0010	0.334	290 (±44)
	25 CaF_2	0.0285	0.0040	0.0020	0.0020	0.0020	0.330	170 (±24)
	30 CaF_2	0.0295	0.0040	0.0030	0.0015	0.0015	0.309	210 (±21)

non-ferrous metallurgical processes [7–10,26–28,33–37]. In a previous study [38], it was concluded that the desulfurization rate by solid phase (CaO, etc.) was too sluggish to be compared to the desulfurization rate by liquid slag. Therefore, the concentration of sulfur in solely liquid slag was deduced by dividing sulfur content in bulk (solid + liquid) slag by the mass fraction of liquid phase, i.e., 0.92 for C/S = 1.7 and 0.98 for C/S = 2.3 system.

To quantitatively express the thermodynamic properties of liquid slag, the sulfide capacity of the solely liquid slag (not the bulk slag) was calculated using FactSage™ 7.3 software and is shown in Fig. 5, which includes the experimental data from a previous study for comparison [26]. The sulfide capacity ($C_{S^{2-}}$) has been used to quantitatively represent the sulfur absorption ability of slag as a function of composition and temperature from a thermodynamic point of view since Fincham and Richardson originally defined it as given in Eqs. (3) and (4) [6,7,11–15,26–28,39–41].

$$\frac{1}{2}S_2(g) + (O^{2-}) = (S^{2-}) + \frac{1}{2}O_2(g) \tag{3}$$

$$C_{S^{2-}} = \frac{K_{(3)} \cdot a_{O^{2-}}}{f_{S^{2-}}} = (\text{wt\%}S^{2-}) \cdot \sqrt{\frac{p_{O_2}}{p_{S_2}}} \tag{4}$$

where $K_{(3)}$ is the gas–slag equilibrium reaction constant of Eq. (3), $a_{O^{2-}}$ is the activity of O^{2-} ion in the slag (i.e., the basicity of the slag), $f_{S^{2-}}$ is the activity coefficient of sulfide ion in the slag (i.e., the stability of sulfide in the slag), and p_i is the partial pressure of the gaseous species i. Thus, the sulfide capacity is a characteristic function of basicity and sulfide ion stability in the slag at a given temperature. In the present study, the oxygen partial pressure ($p_{O_2} = 10^{-14}$ atm) and sulfur partial pressure ($p_{S_2} = 10^{-10}$ atm) were fixed by converting the equilibrium sulfur and oxygen contents in the 316L stainless steel melts from the following thermodynamic data and Wagner formalism, Eq. (7), using interaction parameters listed in Table 3 [42].

$$\frac{1}{2}O_2(g) = [O]_{wt\%} \quad \Delta G^o = -117,150 - 2.9\,T(\text{J/mol}) \tag{5}$$

$$\frac{1}{2}S_2(g) = [S]_{wt\%} \quad \Delta G^o = -135,100 + 23.4\,T(\text{J/mol}) \tag{6}$$

$$log\ a_{i=O,S} = log\ f_{i=O,S} + log[wt\%\ i] = \sum e^j_{i=O,S}[wt\%\ j] + log[wt\%\ i] \tag{7a}$$

where a_i, f_i, and e^j_i represent the Henrian activity and activity coefficient of component $i(=O,S)$ with reference to 1 wt% standard state, and the interaction coefficient between i and j atoms.

In Fig. 5(a), as C/(S + A) ratio increases, the sulfide capacity increases, and previous study data also exhibit the same tendency, whereas the sulfide capacity of slags which have fixed C/(A + S) ratio (=1.5) does not vary according to the increase of the CaF_2 content as shown in Fig. 5(b). Therefore, although 30 wt% CaF_2 was added, since the sulfide capacity (i.e., a driving force of sulfur removal) is constant, the effect of the addition of CaF_2 on the desulfurization efficiency was considered insignificant in view of thermodynamics.

Additionally, despite the similar C/(S + A) ratio, the sulfide capacity of the slag in the previous study (Kang et al. [26]) is

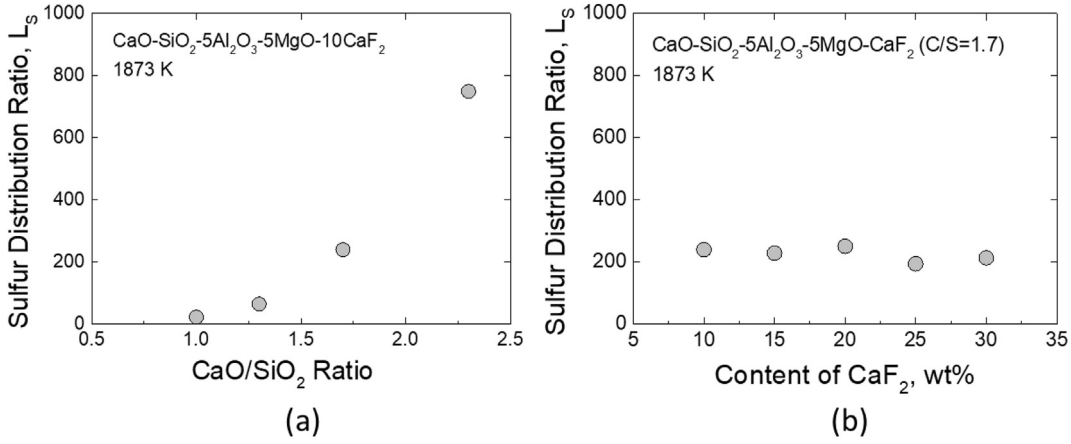

Fig. 4 – Sulfur distribution ratio as a function of (a) CaO/SiO_2 ratio and (b) CaF_2 content in the slag at 1873 K.

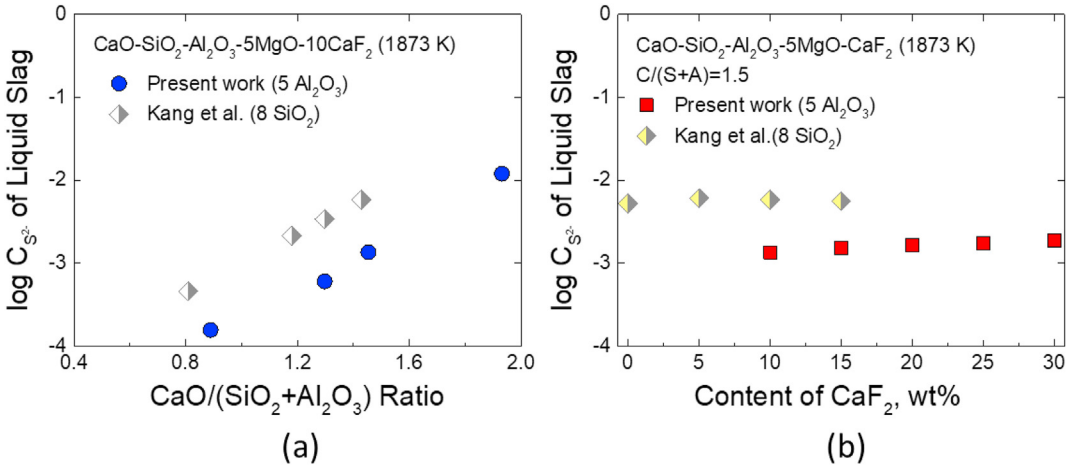

Fig. 5 – Sulfide capacity of the liquid slag as a function of (a) CaO/(SiO_2+Al_2O_3) ratio and (b) CaF_2 content within the slag at 1873 K.

higher than that of the present study. The slag in the present study is calcium silicate–based melts containing 5 wt% Al_2O_3, while the slag of the previous study (Kang et al. [26]) is calcium aluminate–based melts containing 8 wt% SiO_2. Because it is well known that SiO_2 is more acidic than Al_2O_3, the sulfide capacity of the slags in the present study is lower than that of the slags in previous work at a fixed C/(S + A) ratio in Fig. 5.

Combining Eqs. (1) and (3)–(6), the following relationship can be deduced:

$$C_{S^{2-}} = \frac{K_{[1]} \cdot a_{O^{2-}}}{f_{S^{2-}}} = \frac{(\%S^{2-})}{[\%S]} \cdot \frac{a_O}{f_S} = L_S \cdot \frac{a_O}{f_S} \tag{7b}$$

Therefore, the sulfide capacity and sulfur distribution ratio are expected to have a linear correlation to the activity of CaO with a slope of unity on a logarithmic scale assuming that i) the activity of CaO is in proportion to the activity of O^{2-} ion in the slag; and ii) the activity coefficient of sulfide in the slag is not seriously affected by slag composition under dilute condition at a fixed temperature. The sulfide capacity and S distribution ratio according to the activity of CaO is shown in Fig. 6, wherein the $\log C_{s^{2-}}$ and $\log a_{CaO}$ has a linear relationship with a slope of 1.10 ($r^2 = 0.96$) and the same relationship with a slope of 0.93 ($r^2 = 0.95$) is confirmed between $\log L_s$ and $\log a_{CaO}$. From the results shown in Fig. 6, it can be concluded that the desulfurization reaction at the slag-metal interface is in good consistency in view of thermodynamics.

The iso activity lines of CaO at 1873 K, which was calculated using FactSage™ 7.3 software, are shown in Fig. 2. As the C/S ratio increases, a_{CaO} increases, causing an increase in the sulfide capacity and S distribution ratio. However, since a_{CaO} remains the same level even with increasing CaF_2 content, it is considered that this results in the constant $C_{s^{2-}}$ and L_s values as shown in Figs. 4 and 5.

3.1. *Effect of CaO/SiO_2 ratio and CaF_2 content on desulfurization kinetics of STS316L melt*

The overall desulfurization flux equation is given in Eqs. (8) and (9) [22–28,43].

$$J = k_O \left(C_m^b - \frac{C_s^b}{L_S} \right) \tag{8}$$

$$k_O = \frac{1}{\frac{1}{k_m} + \frac{\rho_m}{\rho_s k_s L_s}} \tag{9}$$

where, J, C^b, L_S , ρ, and k_O respectively represent the molar flux of S ($mol \cdot m^{-2} \cdot s^{-1}$), the molar concentration of S in the bulk phase ($mol \cdot m^{-3}$), the S distribution ratio, the density ($kg \cdot m^{-3}$), and the overall mass transfer coefficient ($m \cdot s^{-1}$). Subscripts m and s respectively refer to the metal and slag phase. Here, k_m and k_s were obtained from the experimental data using Eqs. (10) and (11) [22–28,43].

$$-\left(\frac{W_m}{\rho_m A}\right)\left(\frac{[\%S]_o - [\%S]_{eq}}{[\%S]_o}\right) In\left(\frac{[\%S]_t - [\%S]_{eq}}{[\%S]_o - [\%S]_{eq}}\right) = k_m t \tag{10}$$

$$-\left(\frac{W_s}{\rho_s A}\right)\left(\frac{[\%S]_{eq}}{[\%S]_o}\right) In\left(\frac{[\%S]_t - [\%S]_{eq}}{[\%S]_o - [\%S]_{eq}}\right) = k_s t \tag{11}$$

where W, A, [%S], and t, respectively, represent the weight (kg), reaction area (m^2), S concentration (wt%) and reaction time (s). Subscripts o and eq represent initial ($t = 0$) and equilibrium ($t = t_{eq}$) conditions, respectively. In the present study, sulfur in molten steel was rapidly removed within the first 10 min, and the same level of sulfur was observed from 30 to 60 min. Therefore, the equilibrium concentration of sulfur, $[\%S]_{eq}$ in molten steel was taken as an average value of the sulfur concentration measured at 30 min and 60 min. The S concentration in metal and slag, and the S distribution ratio at 60 min are listed in Table 2 and the overall mass transfer

Table 3 – Interaction coefficients e_i^j used in the present calculations [42].

e_i^j (j→)	Cr	Ni	Si	Mn	O	S
i = O	−0.037	0.006	−0.14	−0.03	–	−0.13
i = S	0.011	–	0.063	−0.026	−0.27	−0.028

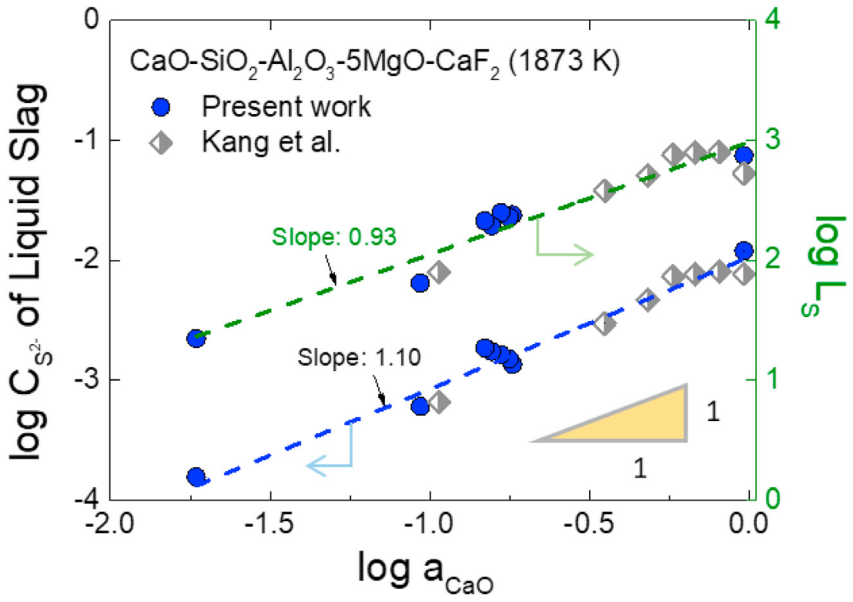

Fig. 6 – Sulfide capacity of the liquid slag and S distribution ratio versus activity of CaO at 1873 K.

coefficients obtained from the experimental data and Eqs. (9)–(11) are shown in Fig. 7.

In Fig. 7(a), the overall mass transfer coefficient k_O increases with increasing C/(S + A) ratio up to a specific level, i.e., C/(S + A) = 1.5 for CaO-SiO_2–based slags from present study, and C/(S + A) = 1.2 for CaO–Al_2O_3–based slags from previous work by Kang et al. [26] After achieving the specific level, a plateau (approx. $logk_O = -4$) was observed. The similar trend is also observed in Fig. 7(b), i.e., the overall mass transfer coefficient is nearly constant although CaF_2 content increases from about 5 to 30 wt% at a fixed C/(S + A) ratio (=1.5) irrespective of slag systems.

From Eq. (9), k_O depends on k_m and k_sL_S, where k_m is approximated as D_m/δ (D_m is diffusion coefficient of sulfur in molten steel, and δ is diffusional boundary layer thickness) from a film theory and is affected by kinetic factors such as the viscosity of steel melt [25,44]. In the present study, because the steel conditions (such as composition, inductive stirring, temperature, etc.) were fixed, k_m was assumed to be constant. Hence, a constant value of k_O indicates that k_m is more dominant factor than k_sL_S in Eq. (9), and the mass transfer of sulfur in metal phase is closer to the desulfurization rate controlling step (RCS). However, a decrease in k_O value at C/(S + A) < 1.5 for CaO-SiO_2–based slags (or < 1.2 for CaO-Al_2O_3–based slags) indicates that the sulfur removal reaction is mainly controlled by slag phase mass transfer and/or metal-slag mixed transportation process, which are strongly influenced by the physicochemical properties of the slag such as viscosity, capacity, etc.

As mentioned above, the specific (or critical) level of C/(S + A) ratio, at which the transition of the RCS of sulfur removal process occurs, is different in CaO-SiO_2–based slags and in CaO-Al_2O_3–based slags in Fig. 7(a). Since SiO_2 is more acidic and network-forming oxide compared to Al_2O_3, the difference in critical level of C/(S + A) ratio in different slags originates from the changes in physicochemical properties of the slags. The more quantitative analysis will be given as follows. Herein the kinetic and the thermodynamic properties

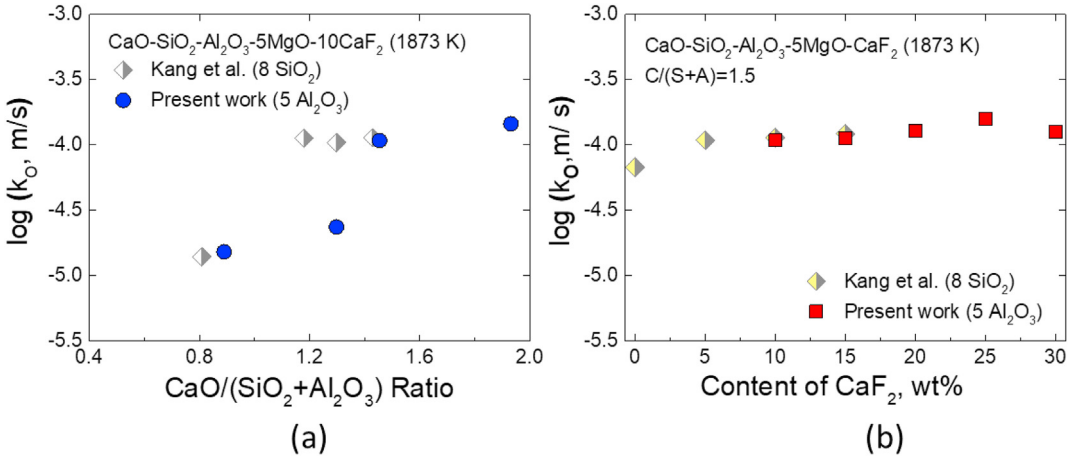

Fig. 7 – Overall mass transfer coefficient as a function of (a) CaO/(SiO_2+Al_2O_3) ratio and (b) CaF_2 content of the slag at 1873 K.

Table 4 – Viscosity of slags (dPa·s) at 1873 K.

Slag conditions		Viscosity of pure liquid slag, η_0	Volume fraction of Solid, f	Apparent viscosity of slag, η
Fixed CaF_2 (=10wt%)	C/S = 1.0	0.94	–	0.94
	C/S = 1.3	0.63	–	0.63
	C/S = 1.7	0.56	0.092	0.84
	C/S = 2.3	0.48	0.034	0.53
Fixed C/(S + A) ratio (=1.5)	15 CaF_2	0.48	–	0.48
	20 CaF_2	0.40	–	0.40
	25 CaF_2	0.34	–	0.34
	30 CaF_2	0.28	–	0.28

are considered to understand the effect of the physicochemical properties of slag upon the desulfurization mechanism.

The viscosity of liquid slag was calculated using FactSage™ 7.3 software to account for the kinetic factor affecting the desulfurization rate and is shown in Table 4. However, because some slags contain solid phase, the apparent viscosity was calculated using the Einstein-Roscoe equation (Eq. (12)), which reflects the effect of solid particle (CaO, Ca_2SiO_4) fractions on slag viscosity [26–28,45–47].

$$\eta = \frac{\eta_0}{(1 - af)^n} \tag{12}$$

where η is the apparent viscosity of multiphase (solid + liquid) slag (dPa·s, poise), η_0 is the viscosity of pure liquid (dPa·s, poise), f is the volume fraction of solid, and a and n are constants. Here, the volume fraction of solid was calculated from the following method: i) Calculate the equilibrium mass fraction of each phase of the mixed slag at the experimental temperature using FactSage software; ii) The density of liquid slag, solid CaO, MgO, and Ca_2SiO_4 was assumed to be 2.65 g/cm^3, 3.34 g/cm^3, 3.58 g/cm^3, and 2.90 g/cm^3, respectively [25,48]; iii) Calculate the volume fraction of solid monoxide (Ca,Mg)O phase (mainly CaO). In Eq. (14), it was assumed that the spherically shaped solid particles were uniformly dispersed, from which $a = 1.35$ and $n = 2.5$ could be taken [26–28,45–50]. The apparent viscosity values calculated from Eq. (12) are listed in Table 4 and Fig. 8.

The viscosity of the present CaO-SiO_2–based slag decreases with increasing C/(S + A) ratio and data from the previous study for CaO-Al_2O_3–based slag also exhibit the same tendency, while the viscosity of the former is slightly higher than that of the latter because of the higher content of SiO_2 in the present slag system. Also, as the CaF_2 content increases, the viscosity of the slag continuously decreases due to the depolymerization of aluminosilicate network structure [16–19]. Comparing the results in Figs. 7(b) and 8(b), it is therefore concluded that CaF_2 addition in the slag of which C/(S + A) = 1.5 does not affect the desulfurization rate controlling step, i.e., metal phase mass transfer. Consequently, the addition of fluorspar at C/(S + A) = 1.5 condition does not helpful to desulfurization rate, whereas the refractory degradation can be occurred, resulting in an increase of operational cost as well as an environmental problem due to fluorine emission [8–10].

The overall mass transfer coefficient (k_O) according to the sulfide capacity of slag ($C_{S^{2-}}$) is shown in Fig. 9(a). Data from previous work are also added for comparison [26]. If the sulfide capacity is above a certain value (i.e., $log\ C_{S^{2-}} > -2.8$), the k_O is almost equivalent, i.e., $log k_O = -4.0(\pm 0.2)$. However, when $log\ C_{S^{2-}}$ is lower than -2.8, the k_O tends to decrease as the sulfide capacity decreases. The k_O values according to the apparent viscosity of the slags are shown in Fig. 9(b). In most cases, the k_O is equivalent, whereas k_O decreases as the viscosity increases greater than a critical value, approx. 0.7 dPa·s (poise).

Meanwhile, the slag phase mass transfer coefficient k_s can be expressed as the following Eq. (13) [21–23,43]:

$$k_s = \frac{D}{\delta} \tag{13}$$

where D and δ respectively represent the diffusion coefficient ($m^2 \cdot s^{-1}$) and diffusion boundary layer (m). Here, the diffusion

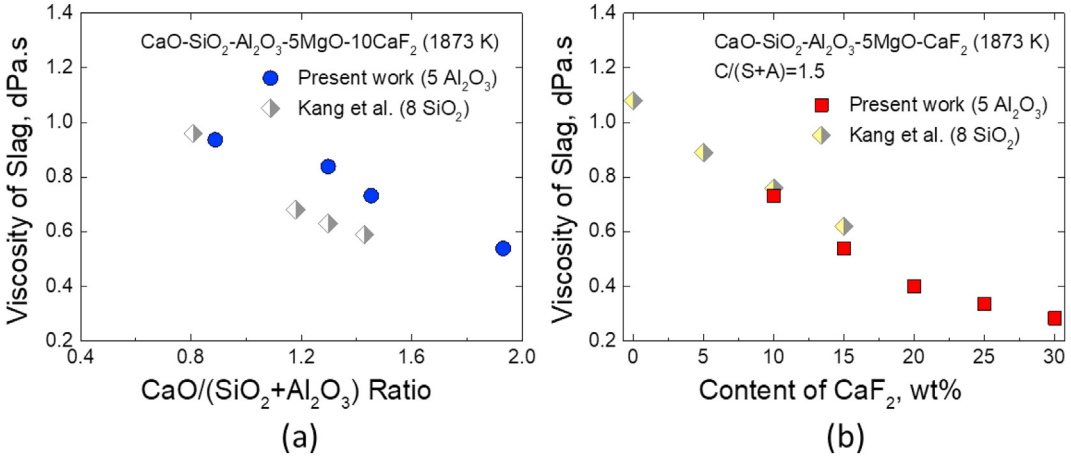

Fig. 8 – Apparent viscosity of the slag as a function of (a) CaO/(SiO_2+Al_2O_3) ratio and (b) CaF_2 content of the slag at 1873 K.

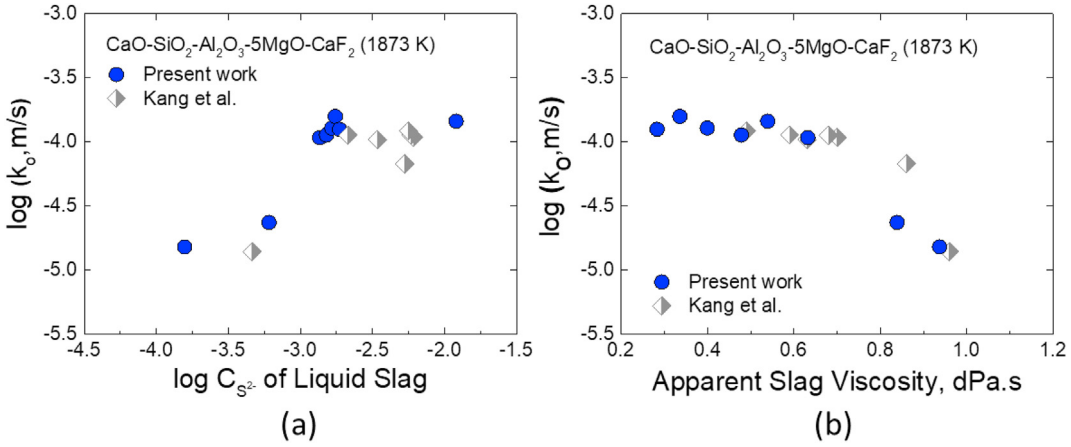

Fig. 9 – Overall mass transfer coefficient as a function of (a) sulfide capacity of the liquid slag and (b) apparent viscosity of the slag at 1873 K.

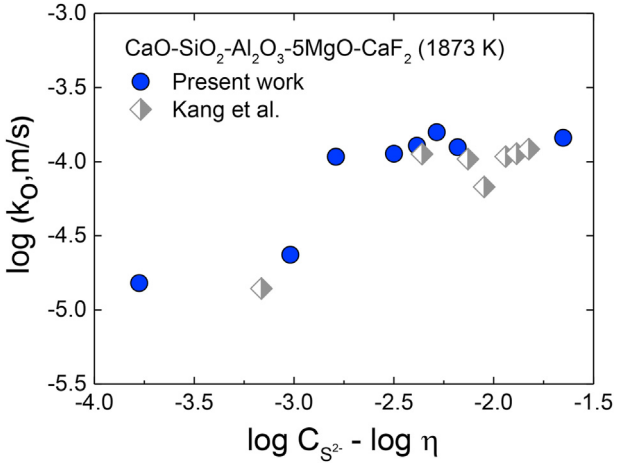

Fig. 10 – Overall mass transfer coefficient as a function of $logC_{S^{2-}} - log\ \eta$ value at 1873 K.

coefficient of sulfur D can be expressed as follows according to the Stokes-Einstein equation (14) [51].

$$D = \frac{k_B T}{6\pi\eta r} \tag{14}$$

where k_B is Boltzmann's constant (1.38×10^{-23} J·K^{-1}), T is temperature (K), η is the viscosity of slag (dPa•s), and r is the radius of the spherical particle (m). From Eq. (14), diffusion coefficient of sulfur D is inversely proportional to slag viscosity at a given temperature, which means that the slag phase mass transfer coefficient k_s are also inversely affected by slag viscosity from Eqs. (13) and (14).

Since the desulfurization process of molten steel has to be considered from both thermodynamic (sulfide capacity) and kinetic (viscosity) factors, the overall mass transfer coefficient can be expressed as a function of '$logC_{S^{2-}} - log\ \eta$' as shown in Fig. 10. The calculated literature values are shown for the sake of comparison [26]. The overall mass transfer coefficient (k_O) increases with the $logC_{S^{2-}} - log\ \eta$ value. However, above a critical value, the k_O is constant.

In the current study, because the k_m is constant, the change of k_O is caused by k_S and L_S. Therefore, the decrease of k_O when the $logC_{S^{2-}} - log\ \eta$ value is less than a critical value due to lower slag basicity represents that the poor physicochemical properties (high viscosity and low sulfide capacity) of the slag negatively affect the desulfurization rate, and the transition of the RCS of the desulfurization reaction from the metal phase mass transfer of sulfur to the slag phase mass transfer or metal-slag mixed mass transfer. However, when the $logC_{S^{2-}} - log\ \eta$ value is greater than a critical value due to higher slag basicity, because the physicochemical properties of slag are satisfactory enough to promote the mass transfer of sulfur in slag phase, the desulfurization reaction is mainly controlled by the mass transfer of sulfur in metal phase.

4. Conclusions

In the present study, desulfurization behavior of Si-killed 316L stainless steel melt with the CaO-SiO_2-CaF_2-Al_2O_3-MgO slag with different CaO/SiO_2 (=C/S) ratio and CaF_2 content at 1873 K was investigated. As the C/S ratio increased from 1.0 to 2.3 (equivalent to C/(S + A) ratio from 0.9 to 1.9), the sulfide capacity and S distribution ratio drastically increased. However, the sulfide capacity and S distribution ratio were not varied irrespective of CaF_2 content at a fixed C/(S + A) = 1.5 ratio. The activity of CaO and sulfide capacity or S distribution ratio exhibited a good linear relationship on a logarithmic scale with a theoretical slope of unity, indicating that the activity of CaO could be a good basicity index. In particular, the constant sulfide capacity with CaF_2 content was originated from the constant activity of CaO as a function of CaF_2 content.

The overall mass transfer coefficient (k_O) increased with C/S ratio but was constant above a certain C/S ratio. The k_O was also constant with variable CaF_2 content. The change in k_O was caused by k_s and/or L_S variation, which was affected by the physicochemical properties of the slag. The rate controlling step (RCS) for sulfur removal reaction *via* high basicity (and CaF_2-containing) slags was confirmed to be metal phase

mass transfer, while the sulfur removal through low basicity slags was controlled by slag phase mass transfer and/or mixed phase mass transportation.

Declaration of Competing Interest

The authors declare that they have no known competing financial interests or personal relationships that could have appeared to influence the work reported in this paper.

Acknowledgments

This work was supported by the Competency Development Program for Industry Specialists from the Korea Institute for Advancement of Technology (KIAT, Grant Number P0002019) and the Korea Evaluation Institute of Industrial Technology (KEIT, Grant Number 20009956), funded by the Ministry of Trade, Industry and Energy (MOTIE), Korea. Also, the authors express their appreciation to the anonymous reviewers' fruitful comments to improve the present article.

REFERENCES

[1] Park JH, Kang Y. Inclusions in stainless steels – a review. Steel Res Int 2017;88(12):1–26. https://doi.org/10.1002/srin.201700130.
[2] Yan P, Huang S, Pandelaers L, Van Dyck J, Guo M, Blanpain B. Effect of the CaO-Al_2O_3-based top slag on the cleanliness of stainless steel during secondary metallurgy. Metall Mater Trans B 2013;44(5):1105–19. https://doi.org/10.1007/s11663-013-9898-5.
[3] Eklund GS. Initiation of pitting at sulfide inclusions in stainless steel. J Electrochem Soc 1974;121(4):467–73. https://doi.org/10.1149/1.2401840.
[4] Bigelow LK, Flemings MC. Sulfide inclusions in steel. Metall Trans B 1976;6(2):275–83. https://doi.org/10.1007/BF02913570.
[5] Maloney JL, Garrison Jr WM. The effect of sulfide type on the fracture behavior of HY180 steel. Acta Mater 2005;53(2):533–51. https://doi.org/10.1016/j.actamat.2004.09.041.
[6] Fincham CJB, Richardson FD. The behaviour of sulphur in silicate and aluminate melts. Proc Roy Soc Lond A 1954;223:40–62. https://doi.org/10.1098/rspa.1954.0099.
[7] Kang YB, Park JH. On the dissolution behavior of sulfur in ternary silicate slags. Metall Mater Trans B 2011;42(6):1211–7. https://doi.org/10.1007/s11663-011-9541-2.
[8] Park JH. Formation of $CaZrO_3$ at the interface between CaO–SiO_2–MgO–CaF_2 (–ZrO_2) slags and magnesia refractories: computational and experimental study. Calphad 2007;31(2):149–54. https://doi.org/10.1016/j.calphad.2007.01.002.
[9] Han JS, Heo JH, Park JH. Interfacial reaction between magnesia refractory and "FeO"-rich slag: formation of magnesiowüstite layer. Ceram Int 2019;45(8):10481–91. https://doi.org/10.1016/j.ceramint.2019.02.110.
[10] Han JS, Kang JG, Shin JH, Chung Y, Park JH. Influence of CaF_2 in calcium aluminate-based slag on the degradation of magnesia refractory. Ceram Int 2018;44(11):13197–204. https://doi.org/10.1016/j.ceramint.2018.04.145.
[11] Bronson A, St Pierre GR. Determination of sulfide capacities of CaO-SiO_2 slags containing CaF_2 and B_2O_3 by an encapsulation method. Metall Trans B 1979;10:375–80. https://doi.org/10.1007/BF02652508.
[12] Susaki K, Maeda M, Sano N. Influence of additives on sulfide capacity of CaO-CaF_2-SiO_2 slags. Metall Mater Trans B 1990;21(6):1081–4. https://doi.org/10.1007/BF02670279.
[13] Hino M, Kitagawa S, Ban-ya S. Sulphide capacities of CaO-Al_2O_3-MgO and CaO-Al_2O_3-SiO_2 slags. ISIJ Int 1993;33(1):36–42. https://doi.org/10.2355/isijinternational.33.36.
[14] Andersson MAT, Jonsson PG, Hallberg M. Optimisation of ladle slag composition by application of sulphide capacity model. Ironmak Steelmak 2000;27(4):286–93. https://doi.org/10.1179/030192300677570.
[15] Cho MK, Cheng J, Park JH, Min DJ. Hot metal desulfurization by CaO–SiO_2–CaF_2–Na_2O slag saturated with MgO. ISIJ Int 2010;50(2):215–21. https://doi.org/10.2355/isijinternational.50.215.
[16] Park JH, Ko KY, Kim TS. Influence of CaF_2 on the viscosity and structure of manganese ferroalloys smelting slags. Metall Mater Trans B 2015;46(2):741–8. https://doi.org/10.1007/s11663-014-0269-7.
[17] Park JH, Min DJ. Carbide capacity of CaO-SiO_2-CaF_2 (-Na_2O) slags at 1773 K. ISIJ Int 2004;44(2):223–8. https://doi.org/10.2355/isijinternational.44.223.
[18] Park JH, Min DJ. The estimation of the iso-viscosity lines in molten CaF_2–CaO–SiO_2 system. ISIJ Int 2007;47(9):1368–9. https://doi.org/10.2355/isijinternational.47.1368. Discussion on.
[19] Kim TS, Park JH. Viscosity-structure relationship of alkaline earth silicate melts containing manganese oxide and calcium fluoride. J Am Ceram Soc 2019;102(8):4943–55. https://doi.org/10.1111/jace.16363.
[20] Goldman KM, Derge G, Philbrook WD. Trans TMS-AIME 1954;200:534–40.
[21] Ramachandran S, King TB, Grant NJ. Trans TMS-AIME 1956;206:1549–53.
[22] Deo B, Grieveson P. Kinetics of desulphurization of molten pig iron. Steel Res 1986;57:514–9.
[23] Deo B, Grieveson P. Desulphurization of molten pig iron containing aluminum by powder injection. Steel Res 1988;59:263–8.
[24] Choi JY, Kim DJ, Lee HG. Reaction kinetics of desulfurization of molten pig iron using CaO–SiO_2–Al_2O_3–Na_2O slag systems. ISIJ Int 2001;41(3):216–24. https://doi.org/10.2355/isijinternational.41.216.
[25] Jung JK, Pak JJ. A kinetic study on desulfurization of molten iron by CaO based slags. J Kor Inst Met Mater 2000;38(4):585–90.
[26] Kang JG, Shin JH, Chung Y, Park JH. Effect of slag chemistry on the desulfurization kinetics in secondary refining processes. Metall Mater Trans B 2017;48(4):2123–35. https://doi.org/10.1007/s11663-017-0948-2.
[27] Jeong TS, Park JH. Effect of fluorspar and industrial wastes (Red mud and Ferromanganese slag) on desulfurization efficiency of molten steel. Metall Mater Trans B 2020;51(5):2309–20. https://doi.org/10.1007/s11663-020-01889-7.
[28] Jeong TS, Oh MK, Chung Y, Park JH. Effect of white mud addition on desulfurization rate of molten steel. Metall Mater Trans B 2021;52(5):3596–605. https://doi.org/10.1007/s11663-021-02343-y.
[29] Yan P, Guo X, Huang S, Van Dyck J, Guo M, Blanpain B. Desulphurisation of stainless steel by using CaO–Al_2O_3 based slags during secondary metallurgy. ISIJ Int 2013;53(3):459–67. https://doi.org/10.2355/isijinternational.53.459.

[30] Park JH, Kim DS. Effect of CaO-Al_2O_3-MgO slags on the formation of MgO-Al_2O_3 inclusions in ferritic stainless steel. Metall Mater Trans B 2005;36(4):495–502. https://doi.org/10.1007/s11663-005-0041-0.
[31] Yin X, Sun Y, Yang Y, Deng X, Barati M, McLean A. Effect of alloy addition on inclusion evolution in stainless steels. Iornmaking & Steelmaking 2017;44(2):152–8. https://doi.org/10.1080/03019233.2016.1185285.
[32] Ren Y, Zhang L, Fang W, Shao S, Yang J, Mao W. Effect of slag composition on inclusions in Si-deoxidized 18Cr-8Ni stainless steels. Metall Mater Trans B 2016;47(2):1024–34. https://doi.org/10.1007/s11663-015-0554-0.
[33] Park JH, Todoroki H. Control of MgO·Al_2O_3 spinel inclusions in stainless steels. ISIJ Int 2010;50(10):1333–46. https://doi.org/10.2355/isijinternational.50.1333.
[34] Park JH, Jung IH, Lee SB. Phase diagram study for the CaO-SiO_2-Cr_2O_3-5 mass.% MgO-10 mass.% MnO system. Met Mater Int 2009;15(4):677–81. https://doi.org/10.1007/s12540-009-0677-4.
[35] Shin JH, Park JH. Modification of inclusions in molten steel by Mg-Ca transfer from top slag: experimental confirmation of the 'refractory-slag-metal-inclusion (ReSMI)'multiphase reaction model. Metall Mater Trans B 2017;48(6):2820–5. https://doi.org/10.1007/s11663-017-1080-z.
[36] Piva SPT, Kumar D, Pistorius PC. Modeling manganese silicate inclusion composition changes during ladle treatment using FactSage macros. Metall Mater Trans B 2017;48(1):37–45. https://doi.org/10.1007/s11663-016-0764-0.
[37] Sineva S, Shevchenko M, Shishin D, Hidayat T, Chen J, Hayes PC, et al. JOM 2020;72(10):3401–9. https://doi.org/10.1007/s11837-020-04326-x.
[38] Takahashi K, Utagawa K, Shibata H, Kitamura S, Kikuchi N, Kishimoto Y. Influence of solid CaO and liquid slag on hot metal desulfurization. ISIJ Int 2012;52(1):10–7. https://doi.org/10.2355/isijinternational.52.10.
[39] Kang YB, Pelton AD. Thermodynamic model and database for sulfides dissolved in molten oxide slags. Metall Mater Trans B 2009;40(6):979–94. https://doi.org/10.1007/s11663-009-9283-6.
[40] Lee S, Min DJ. Investigation of sulfide capacity of aluminosilicate slag based on ionic structure considerations. J Am Ceram Soc 2018;101(2):634–43. https://doi.org/10.1111/jace.15227.
[41] Allertz C, Sichen D. Sulfide capacity in ladle slag at steelmaking temperatures. Metall Mater Trans B 2015;46(6):2609–15. https://doi.org/10.1007/s11663-015-0444-5.
[42] Gaye HR. In: Cramb AW, editor. The making, shaping and treating of steel. 11th ed. Pittsburgh: The AISE Steel Foundation; 2003. Casting Volume, [Chapter 3] (Inclusion Formation in Steels).
[43] Deo B, Boom R. Fundamentals of steelmaking metallurgy. New Tork: Prentice Fall; 1993.
[44] Cho JH, Martinsson J, Sichen D, Park JH. Desulfurization behavior of Incoloy® 825 superalloy by CaO-Al_2O_3-MgO-TiO_2 slag. Metall Mater Trans B 2021;52(6):3660–70. https://doi.org/10.1007/s11663-021-02338-9.
[45] Einstein A. Eine neue bestimmung der moleküldimensionen. Ann Phys 1906;19:289–306. https://doi.org/10.1002/andp.19063240204.
[46] Roscoe R. The viscosity of suspensions of rigid spheres. Br J Appl Phys 1952;3(8):267–9.
[47] Seok SH, Jung SM, Lee YS, Min DJ. Viscosity of highly basic slags. ISIJ Int 2007;47(8):1090–6. https://doi.org/10.2355/isijinternational.47.1090.
[48] Hynes WM. CRC handbook of chemistry and physics. 92nd ed. Boca Raton: CRC Press, Taylor and Francis; 2011.
[49] Pezzin RO, Berger APL, Grillo FF, Junca E, Furtado HS, Oliveira JR. Analysis of the influence of the solid and liquid phases on steel desulfurization with slags from the CaO–Al_2O_3 systems using computational thermodynamics. J Mater Res Technol 2020;991:836–46. https://doi.org/10.1016/j.jmrt.2019.11.023.
[50] Wang HY, Zhang GH, Chou KC. Preparation of low-carbon and low-sulfur Fe-Cr-Ni-Si alloy by using $CaSO_4$-containing stainless steel pickling sludge. Metall Mater Trans B 2020;51(5):2057–67. https://doi.org/10.1007/s11663-020-01922-9.
[51] Einstein A. Über die von der molekularkinetischen Theorie der Wärme geforderte Bewegung von in ruhenden Flüssigkeiten suspendierten Teilchen. Ann Phys 1905;17:549–60. https://doi.org/10.1002/andp.19053220806.